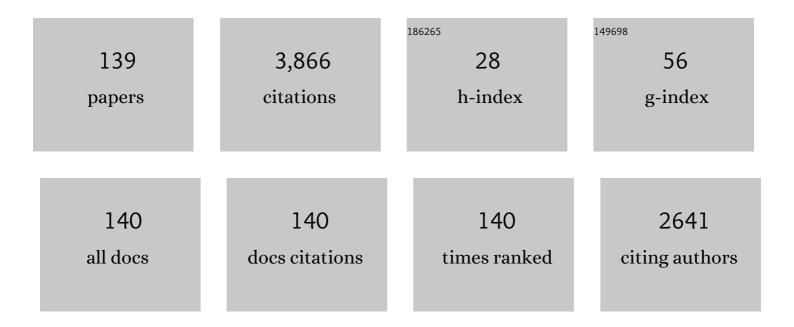
List of Publications by Year in descending order

Source: https://exaly.com/author-pdf/1485840/publications.pdf Version: 2024-02-01



#	Article	IF	CITATIONS
1	Dry-sliding tribological properties of AlCoCrFeNiTi0.5 high-entropy alloy. Rare Metals, 2022, 41, 4266-4272.	7.1	7
2	Local orders, lattice distortions, and electronic structure dominated mechanical properties of (ZrHfTaM1M2)C (M = Nb, Ti, V). Journal of the American Ceramic Society, 2022, 105, 4260-4276.	3.8	8
3	Tailoring the magnetic properties and microstructure of Alnico 8 magnets by various Ti contents and processing conditions. Intermetallics, 2022, 143, 107486.	3.9	8
4	Liquid state dependent solidification of a Co-B eutectic alloy under a high magnetic field. Journal of Materials Science and Technology, 2022, 116, 58-71.	10.7	3
5	Formation of core-shell structure in immiscible CoCrCuFe1.5Ni0.5 high-entropy alloy. Materials Letters, 2022, , 132452.	2.6	2
6	Effect of long-term aging treatment on the tensile strength and ductility of GH 605 superalloy. Progress in Natural Science: Materials International, 2022, 32, 375-384.	4.4	4
7	Tailoring mechanical and magnetic properties of AlCoCrFeNi high-entropy alloy via phase transformation. Journal of Materials Science and Technology, 2021, 73, 83-90.	10.7	34
8	Microstructure evolution of peritectic Al–18 at.% Ni alloy directionally solidified in high magnetic fields. Journal of Materials Science and Technology, 2021, 76, 51-59.	10.7	11
9	Microstructure and properties of AlCoCrCuFeNi high-entropy alloy solidified under high magnetic field. Materials Letters, 2021, 285, 129182.	2.6	10
10	Investigation of atomic diffusion at Ni/Zr 48 Cu 36 Ag 8 Al 8 interfaces in the glass transition temperature. Surface and Interface Analysis, 2021, 53, 135-139.	1.8	1
11	Tailoring the microstructure, magnetic properties and interaction mechanisms of Alnico-Ta alloys by magnetic field treatment. Journal of Alloys and Compounds, 2021, 857, 157586.	5.5	14
12	Integrating data mining and machine learning to discover high-strength ductile titanium alloys. Acta Materialia, 2021, 202, 211-221.	7.9	85
13	Thermal–Mechanical Processing and Strengthen in AlxCoCrFeNi High-Entropy Alloys. Frontiers in Materials, 2021, 7, .	2.4	8
14	Solidification of Immiscible Alloys under High Magnetic Field: A Review. Metals, 2021, 11, 525.	2.3	6
15	Effect of High Strain Rate on Adiabatic Shearing of $\hat{I} \pm + \hat{I}^2$ Dual-Phase Ti Alloy. Materials, 2021, 14, 2044.	2.9	3
16	Hot Deformation and Subsequent Annealing on the Microstructure and Hardness of an Al0.3CoCrFeNi High-entropy Alloy. Acta Metallurgica Sinica (English Letters), 2021, 34, 1527-1536.	2.9	17
17	Nanophase precipitation and strengthening in a dual-phase Al0.5CoCrFeNi high-entropy alloy. Journal of Materials Science and Technology, 2021, 72, 1-7.	10.7	51
18	Electronic structures and properties of TiAl/Ti2AlNb heterogeneous interfaces: A comprehensive first-principles study. Intermetallics, 2021, 133, 107173.	3.9	15

#	Article	IF	CITATIONS
19	Revealing the Local Microstates of Fe–Mn–Al Medium Entropy Alloy: A Comprehensive First-principles Study. Acta Metallurgica Sinica (English Letters), 2021, 34, 1492-1502.	2.9	2
20	The Localized Corrosion and Stress Corrosion Cracking of a 6005A-T6 Extrusion Profile. Materials, 2021, 14, 4924.	2.9	1
21	Optimizing mechanical and magnetic properties of AlCoCrFeNi high-entropy alloy via FCC to BCC phase transformation. Journal of Materials Science and Technology, 2021, 86, 117-126.	10.7	27
22	Coupling effects of high magnetic field and annealing on the microstructure evolution and mechanical properties of additive manufactured Ti–6Al–4V. Materials Science & Engineering A: Structural Materials: Properties, Microstructure and Processing, 2021, 824, 141815.	5.6	18
23	Effect of high magnetic field assisted heat treatment on microstructure and properties of AlCoCrCuFeNi high-entropy alloy. Materials Letters, 2021, 303, 130540.	2.6	11
24	Effects of an ultra-high magnetic field up to 25 T on the phase transformations of undercooled Co-B eutectic alloy. Journal of Materials Science and Technology, 2021, 93, 79-88.	10.7	6
25	Lattice distortion-enhanced superlubricity of (Mo, X)S <sub>2</sub> (X = Al, Ti, Cr and V) with moiré superlattice. Nanoscale, 2021, 13, 16234-16243.	5.6	6
26	Evolution of microstructure and hardness in a dual-phase Al0.5CoCrFeNi high-entropy alloy with different grain sizes. Rare Metals, 2020, 39, 156-161.	7.1	25
27	Microstructure and Mechanical Properties of CoCrFeMnNiSnx High-Entropy Alloys. Metals and Materials International, 2020, 26, 292-301.	3.4	27
28	Magnetic-field-induced chain-like assemblies of the primary phase during non-equilibrium solidification of a Co-B eutectic alloy: Experiments and modeling. Journal of Alloys and Compounds, 2020, 815, 152446.	5.5	12
29	Effect of strong magnetic field on the microstructure and mechanical-magnetic properties of AlCoCrFeNi high-entropy alloy. Journal of Alloys and Compounds, 2020, 820, 153407.	5.5	34
30	Liquidâ^'liquid structure transition in metallic melt and its impact on solidification: A review. Transactions of Nonferrous Metals Society of China, 2020, 30, 2293-2310.	4.2	15
31	The cryogenic mechanical property deviation of Ti-based bulk metallic glass composite induced by interstitial element. Journal of Non-Crystalline Solids, 2020, 542, 120105.	3.1	3
32	High-throughput investigations of configurational-transformation-dominated serrations in CuZr/Cu nanolaminates. Journal of Materials Science and Technology, 2020, 53, 192-199.	10.7	14
33	Influence of high magnetic field on the liquid-liquid phase separation behavior of an undercooled Cu–Co immiscible alloy. Journal of Alloys and Compounds, 2020, 842, 155502.	5.5	24
34	Enhancing mechanical properties of Al0.25CoCrFeNi high-entropy alloy via cold rolling and subsequent annealing. Journal of Alloys and Compounds, 2020, 830, 154645.	5.5	25
35	Liquid-liquid phase separation in immiscible Cu-Co alloy. Materials Letters, 2020, 268, 127585.	2.6	11
36	Revealing foundations of the intergranular corrosion of 5XXX and 6XXX Al alloys. Materials Letters, 2020. 271. 127767.	2.6	15

#	Article	IF	CITATIONS
37	Oxygen-Induced Mechanical Property Variations of Rapidly Solidified Ti-Based Bulk Metallic Composites. Journal of Materials Engineering and Performance, 2019, 28, 5793-5796.	2.5	0
38	When a defect is a pathway to improve stability: a case study of the L12 Co3TM superlattice intrinsic stacking fault. Journal of Materials Science, 2019, 54, 13609-13618.	3.7	16
39	A new microscopic coordinated deformation model of Ti-based bulk metallic composites during tensile deformation. Scripta Materialia, 2019, 172, 23-27.	5.2	6
40	A novel strategy for enhancing mechanical performance of Al0.5CoCrFeNi high-entropy alloy via high magnetic field. Materials Letters, 2019, 240, 250-252.	2.6	8
41	Composition dependent characteristic transition temperatures of Co-B melts. Journal of Non-Crystalline Solids, 2019, 522, 119583.	3.1	8
42	Pitting Corrosion of Natural Aged Al–Mg–Si Extrusion Profile. Materials, 2019, 12, 1081.	2.9	7
43	Fully Recrystallized Al0.5CoCrFeNi High-Entropy Alloy Strengthened by Nanoscale Precipitates. Metals and Materials International, 2019, 25, 1145-1150.	3.4	24
44	Local lattice distortion mediated formation of stacking faults in Mg alloys. Acta Materialia, 2019, 170, 231-239.	7.9	45
45	Effect of Mn Addition on the Microstructures and Mechanical Properties of CoCrFeNiPd High Entropy Alloy. Entropy, 2019, 21, 288.	2.2	4
46	Interstitial triggered grain boundary embrittlement of Al–X (X = H, N and O). Computational Materials Science, 2019, 163, 241-247.	3.0	8
47	The effect of high magnetic field on the microstructure evolution of a Cu-Co alloy during non-equilibrium solidification. Journal of Crystal Growth, 2019, 515, 78-82.	1.5	9
48	Outstanding tensile properties of a precipitation-strengthened FeCoNiCrTi0.2 high-entropy alloy at room and cryogenic temperatures. Acta Materialia, 2019, 165, 228-240.	7.9	373
49	Tensile properties and deformation micromechanism of Ti-based metallic glass composite containing impurity elements. Journal of Alloys and Compounds, 2019, 784, 220-230.	5.5	14
50	Nucleation of supercooled Co melts under a high magnetic field. Materials Chemistry and Physics, 2019, 225, 133-136.	4.0	22
51	Corrosive and tribological behaviors of AlCoCrFeNi-M high entropy alloys under 90 wt. % H2O2 solution. Tribology International, 2019, 131, 24-32.	5.9	32
52	Temperature-induced structure transition in a liquid Co-B eutectic alloy. Materials Letters, 2019, 234, 351-353.	2.6	10
53	Numerical Simulation and Process Optimization of Vacuum Investment Casting for Be–Al Alloys. International Journal of Metalcasting, 2019, 13, 74-81.	1.9	15
54	Soldering of Zr-based bulk metallic glass and copper by Au–12Ge eutectic alloy. Rare Metals, 2019, 38, 52-58.	7.1	1

#	Article	IF	CITATIONS
55	Insight into solid-solution strengthened bulk and stacking faults properties in Ti alloys: a comprehensive first-principles study. Journal of Materials Science, 2018, 53, 7493-7505.	3.7	17
56	Obligatory and facilitative allelic variation in the DNA methylome within common disease-associated loci. Nature Communications, 2018, 9, 8.	12.8	107
57	Temperature dependent deformation mechanisms of Al0.3CoCrFeNi high-entropy alloy, starting from serrated flow behavior. Journal of Alloys and Compounds, 2018, 757, 39-43.	5.5	22
58	Microstructure and mechanical properties of non-equilibrium solidified CoCrFeNi high entropy alloy. Materials Chemistry and Physics, 2018, 210, 192-196.	4.0	57
59	Microstructure characterization of CoCrFeNiMnPd eutectic high-entropy alloys. Journal of Alloys and Compounds, 2018, 731, 600-611.	5.5	49
60	Effect of Cold Rolling on the Phase Transformation Kinetics of an Al0.5CoCrFeNi High-Entropy Alloy. Entropy, 2018, 20, 917.	2.2	13
61	Phase Transformation Kinetics of a FCC Al0.25CoCrFeNi High-Entropy Alloy during Isochronal Heating. Metals, 2018, 8, 1015.	2.3	4
62	Effect of strong static magnetic field on the microstructure and transformation temperature of Co–Ni–Al ferromagnetic shape memory alloy. Journal of Materials Science: Materials in Electronics, 2018, 29, 19491-19498.	2.2	5
63	Microstructure and properties of bulk Al0.5CoCrFeNi high-entropy alloy by cold rolling and subsequent annealing. Materials Science & Engineering A: Structural Materials: Properties, Microstructure and Processing, 2018, 729, 141-148.	5.6	74
64	Transition from hypereutectic to hypoeutectic for rapid solidification in an undercooled Co-B alloy. Journal of Crystal Growth, 2018, 499, 98-105.	1.5	9
65	Effect of Solidification on Microstructure and Properties of FeCoNi(AlSi)0.2 High-Entropy Alloy Under Strong Static Magnetic Field. Entropy, 2018, 20, 275.	2.2	9
66	Seaweed eutectic-dendritic solidification pattern in a CoCrFeNiMnPd eutectic high-entropy alloy. Intermetallics, 2017, 85, 74-79.	3.9	55
67	Tune the mechanical properties of Ti-based metallic glass composites by additions of nitrogen. Materials Science & Engineering A: Structural Materials: Properties, Microstructure and Processing, 2017, 694, 93-97.	5.6	13
68	Liquid–liquid structure transition and nucleation in undercooled Co-B eutectic alloys. Applied Physics A: Materials Science and Processing, 2017, 123, 1.	2.3	27
69	The characteristics of serration in Al0.5CoCrFeNi high entropy alloy. Materials Science & Engineering A: Structural Materials: Properties, Microstructure and Processing, 2017, 702, 96-103.	5.6	62
70	Liquid-phase separation in undercooled CoCrCuFeNi high entropy alloy. Intermetallics, 2017, 86, 110-115.	3.9	30
71	The FCC to BCC phase transformation kinetics in an Al0.5CoCrFeNi high entropy alloy. Journal of Alloys and Compounds, 2017, 710, 144-150.	5.5	59
72	Formation of a hexagonal closed-packed phase in Al0.5CoCrFeNi high entropy alloy. MRS Communications, 2017, 7, 879-884.	1.8	16

#	Article	IF	CITATIONS
73	Strong magnetic field effect on the nucleation of a highly undercooled Co-Sn melt. Scientific Reports, 2017, 7, 4958.	3.3	18
74	Heterogeneous precipitation behavior and stacking-fault-mediated deformation in a CoCrNi-based medium-entropy alloy. Acta Materialia, 2017, 138, 72-82.	7.9	553
75	Dendrite size dependence of mechanical properties of in-situ Ti-based bulk metallic glass matrix composites. Materials Science & Engineering A: Structural Materials: Properties, Microstructure and Processing, 2017, 704, 77-81.	5.6	17
76	Instability Pattern Formation in a Liquid Metal under High Magnetic Fields. Scientific Reports, 2017, 7, 2248.	3.3	9
77	The Effect of Thermal Cycling Treatments on the Thermal Stability and Mechanical Properties of a Ti-Based Bulk Metallic Glass Composite. Metals, 2016, 6, 274.	2.3	10
78	Hot Deformation Behavior of As-Cast and Homogenized Al0.5CoCrFeNi High Entropy Alloys. Metals, 2016, 6, 277.	2.3	26
79	Relationship between grain boundary diffusion in nanocrystals and amorphous microstructure. Surface and Interface Analysis, 2016, 48, 1341-1344.	1.8	1
80	Quasi-static and dynamic deformation of an in-situ Ti-based metallic glass composite in supercooled liquid region. Journal of Alloys and Compounds, 2016, 679, 239-246.	5.5	12
81	Deformation behavior of a Ti-based bulk metallic glass composite in the supercooled liquid region. Materials and Design, 2016, 90, 595-600.	7.0	13
82	Size-dependent role of S phase in pitting initiation of 2024Al alloy. Corrosion Science, 2016, 105, 183-189.	6.6	60
83	Tribological Behavior of 1Cr18Ni9Ti Steel under Hydrogen Peroxide Solution against Different Ceramic Counterparts. Rare Metal Materials and Engineering, 2016, 45, 593-598.	0.8	3
84	EFFECT OF HEATING TYPES ON THE UNDERCOOLED SOLIDIFICATION MICROSTRUCTURE OF Co76Sn24EUTECTIC ALLOY. , 2016, , 649-656.		0
85	Phase Separation and Microstructure Evolution of Zr48Cu36Ag8Al8 Bulk Metallic Glass in the Supercooled Liquid Region. Rare Metal Materials and Engineering, 2016, 45, 567-570.	0.8	15
86	Tensile deformation mechanisms of an in-situ Ti-based metallic glass matrix composite at cryogenic temperature. Scientific Reports, 2016, 6, 32287.	3.3	18
87	Reexaminations of the effects of magnetic field on the nucleation of undercooled Cu melt. Japanese Journal of Applied Physics, 2016, 55, 105601.	1.5	11
88	Diffusion Bonding between Zr-Based Metallic Glass and Copper. Rare Metal Materials and Engineering, 2016, 45, 42-45.	0.8	11
89	Strengthening of nanoprecipitations in an annealed Al0.5CoCrFeNi high entropy alloy. Materials Science & Engineering A: Structural Materials: Properties, Microstructure and Processing, 2016, 671, 82-86.	5.6	158
90	Numerical modeling and experiment of counter-gravity casting for titanium alloys. International Journal of Advanced Manufacturing Technology, 2016, 85, 1877-1885.	3.0	7

#	Article	IF	CITATIONS
91	Effect of liquid–liquid structure transition on the nucleation in undercooled Co–Sn eutectic alloy. Materials Chemistry and Physics, 2016, 170, 261-265.	4.0	13
92	Enhanced mechanical properties of a CoCrFeNi high entropy alloy by supercooling method. Materials and Design, 2016, 95, 183-187.	7.0	99
93	Deformation behaviors of a Ti-based bulk metallic glass composite in the dendrite softening region. Materials Science & Engineering A: Structural Materials: Properties, Microstructure and Processing, 2016, 653, 1-7.	5.6	8
94	Tribological Behavior of AlCoCrFeNi(Ti0.5) High Entropy Alloys under Oil and MACs Lubrication. Journal of Materials Science and Technology, 2016, 32, 470-476.	10.7	61
95	Thermal Stability and the Matrix Induced Brittleness in a Ti-based Bulk Metallic Glass Composite. Materials Research, 2015, 18, 83-88.	1.3	5
96	Diffusion behavior of Ni in Zr48Cu36Ag8Al8 bulk metallic glass within supercooled liquid region. Transactions of Nonferrous Metals Society of China, 2015, 25, 1171-1175.	4.2	3
97	Microstructure Evolution and Mechanical Properties of a Ti-Based Bulk Metallic Glass Composite. Journal of Materials Engineering and Performance, 2015, 24, 2354-2358.	2.5	7
98	Magnetic field enhanced phase precipitation in an undercooled Co–Sn alloy. Materials Letters, 2015, 139, 288-291.	2.6	18
99	Evidence for the structure transition in a liquid Co–Sn alloy by in-situ magnetization measurement. Materials Letters, 2015, 145, 261-263.	2.6	10
100	Enhanced mechanical properties of Ti-based metallic glass composites prepared under medium vacuum system. Journal of Non-Crystalline Solids, 2015, 413, 15-19.	3.1	10
101	Microstructure Evolution of a Ti-Based Bulk Metallic Glass Composite During Deformation. Journal of Materials Engineering and Performance, 2015, 24, 748-753.	2.5	9
102	Temperature dependent dynamic flow behavior of an in-situ Ti-based bulk metallic glass composite. Materials Science & Engineering A: Structural Materials: Properties, Microstructure and Processing, 2015, 627, 21-26.	5.6	7
103	Experimental platform for solidification and <i>in-situ</i> magnetization measurement of undercooled melt under strong magnetic field. Review of Scientific Instruments, 2015, 86, 025102.	1.3	19
104	Anomalous structural dynamics in liquid Al80Cu20: An ab initio molecular dynamics study. Acta Materialia, 2015, 97, 75-85.	7.9	62
105	Tribological behavior of AlCoCrCuFeNi and AlCoCrFeNiTi0.5 high entropy alloys under hydrogen peroxide solution against different counterparts. Tribology International, 2015, 92, 203-210.	5.9	39
106	Correlation between diffusion and crystallization behaviors in Ni/Zr48Cu36Ag8Al8 diffusion couple. Journal of Non-Crystalline Solids, 2015, 417-418, 34-38.	3.1	5
107	Strain-rate-dependent deformation behavior in a Ti-based bulk metallic glass composite upon dynamic deformation. Journal of Alloys and Compounds, 2015, 639, 131-138.	5.5	28
108	Dynamic mechanical properties of a Ti-based metallic glass matrix composite. Journal of Applied Physics, 2015, 117, 155102.	2.5	3

#	Article	IF	CITATIONS
109	Overheating dependent undercooling in a hypoeutectic Co–B alloy. Materials Chemistry and Physics, 2015, 149-150, 17-20.	4.0	12
110	Multiple twins of a decagonal approximant embedded in S-Al2CuMg phase resulting in pitting initiation of a 2024Al alloy. Acta Materialia, 2015, 82, 22-31.	7.9	59
111	Characterization of BCC phases in AlCoCrFeNiTix high entropy alloys. Materials Letters, 2015, 138, 78-80.	2.6	103
112	Interface characteristics of a Zr-based BMG/copper laminated composite. Surface and Interface Analysis, 2014, 46, 61-64.	1.8	7
113	Strain rate response of a Ti-based metallic glass composite at cryogenic temperature. Materials Letters, 2014, 117, 228-230.	2.6	18
114	Effect of a weak transverse magnetic field on solidification structure during directional solidification. Acta Materialia, 2014, 64, 367-381.	7.9	67
115	Microstructure and Tribological Properties of AlCoCrFeNiTi0.5 High-Entropy Alloy in Hydrogen Peroxide Solution. Metallurgical and Materials Transactions A: Physical Metallurgy and Materials Science, 2014, 45, 201-207.	2.2	49
116	Anomalous magnetism and normal field instability in supercooled liquid cobalt. Applied Physics Letters, 2014, 105, 144101.	3.3	16
117	Structure transitions near liquidus and the nucleation of undercooled melt of Ni–Cr–W superalloy. Physica B: Condensed Matter, 2014, 454, 8-14.	2.7	4
118	Crystallization kinetics of Cu38Zr46Ag8Al8 bulk metallic glass in different heating conditions. Journal of Non-Crystalline Solids, 2014, 404, 7-12.	3.1	35
119	Study on Structural Transformation Behavior of a Ti-Based Bulk Metallic Glass by Thermal Expansion Method. Rare Metal Materials and Engineering, 2014, 43, 1047-1050.	0.8	4
120	Rheological behavior of Cu–Zr-based metallic glass in the supercooled liquid region. Journal of Alloys and Compounds, 2014, 592, 189-195.	5.5	18
121	Deformation behavior of a Ti-based bulk metallic glass composite with excellent cryogenic mechanical properties. Materials & Design, 2014, 53, 737-740.	5.1	26
122	Pure-Shuffle Nucleation of Deformation Twins in Hexagonal-Close-Packed Metals. Materials Research Letters, 2013, 1, 126-132.	8.7	181
123	Diffusion Bonding of Fe-Based Amorphous Ribbon to Crystalline Cu. Materials Science Forum, 2013, 745-746, 788-792.	0.3	1
124	Interactions Between TiAl Melt and Crucibles Material during Casting Process. , 2013, , 2669-2678.		0
125	Crystallization and compressive behaviors of Ti40Zr25Ni8Cu9Be18 BMG cast from different liquid states. Intermetallics, 2012, 28, 45-50.	3.9	9
126	Influence of oxygen on microstructure and phase transformation in high Nb containing TiAl alloys. Materials Letters, 2012, 83, 198-201.	2.6	12

#	Article	IF	CITATIONS
127	Enthalpy recovery and its effect on homogeneous flow stress during supercooled liquid region for Ti40Zr25Ni8Cu9Be18 bulk metallic glass. Journal of Non-Crystalline Solids, 2011, 357, 3049-3052.	3.1	1
128	Correlations between Shear Bands and Plasticity in Ti-Based Bulk Metallic Glass. Rare Metal Materials and Engineering, 2011, 40, 399-402.	0.8	6
129	The Nanocrystal and Its Thermal Stability in Ti <sub>40</sub> Zr <sub>25</sub> Ni <sub>8</sub> Cu <sub>9</sub> Be <sub>18</sub> Metallic Glass during Homogeneous Deformation. Materials Science Forum, 2011, 688, 431-436.	0.3	0
130	Limitation of the Johnson-Mehl-Avrami equation for the kinetic analysis of crystallization in a Ti-based amorphous alloy. International Journal of Minerals, Metallurgy and Materials, 2010, 17, 307-311.	4.9	4
131	Microstructure Changes in Zr-Based Metallic Glass Induced by Ion Milling. Rare Metal Materials and Engineering, 2010, 39, 1693-1696.	0.8	4
132	Formation of Stress-Induced Nano Defects in Shear Bands of Metallic Glasses. Rare Metal Materials and Engineering, 2010, 39, 941-944.	0.8	5
133	Microstructure, phase and microhardness distribution of laser-deposited Ni-based amorphous coating. International Journal of Surface Science and Engineering, 2010, 4, 296.	0.4	10
134	On discussion of the applicability of local Avrami exponent: Errors and solutions. Materials Letters, 2009, 63, 1153-1155.	2.6	20
135	An integral fitting method for analyzing the isochronal transformation kinetics: Application to the crystallization of a Ti-based amorphous alloy. Journal of Physics and Chemistry of Solids, 2009, 70, 1448-1453.	4.0	16
136	Kinetic analysis of the isochronal crystallization of Ti40Zr25Ni8Cu9Be18 metallic glass. Journal of Non-Crystalline Solids, 2009, 355, 420-424.	3.1	13
137	Effect of the kinetic model on parameter distortions in non-isothermal transformations. Journal of Alloys and Compounds, 2009, 479, L22-L25.	5.5	2
138	Determination of kinetic parameters during isochronal crystallization of Ti40Zr25Ni8Cu9Be18 metallic glass. Journal of Alloys and Compounds, 2009, 479, 835-839.	5.5	20
139	Deformation Micromechanisms of a Ti-Based Metallic Glass Composite with Excellent Mechanical Properties. Materials Science Forum, 0, 745-746, 809-814.	0.3	2